Brain Small-Worldness Properties and Perceived Fatigue in Mild Cognitive Impairment

Article *in* The Journals of Gerontology Series A Biological Sciences and Medical Sciences · March 2021

DOI: 10.1093/gerona/glab084

6 authors, including:

Mia Anthony
University of Rochester
11 PUBLICATIONS **58** CITATIONS
SEE PROFILE

Timothy M Baran
University of Rochester
57 PUBLICATIONS **295** CITATIONS
SEE PROFILE

THE GERONTOLOGICAL SOCIETY OF AMERICA®

Journals of Gerontology: Medical Sciences
cite as: *J Gerontol A Biol Sci Med Sci*, 2021, Vol. XX, No. XX, 1–6
doi:10.1093/gerona/glab084
Advance Access publication March 18, 2021

OXFORD

Research Report

Brain Small-Worldness Properties and Perceived Fatigue in Mild Cognitive Impairment

Bennett Kukla, BS,[1,†] Mia Anthony, BS,[2,†] Shuyi Chen, BS,[2,†] Adam Turnbull, PhD,[3,4] Timothy M. Baran, PhD,[3] and Feng V. Lin, PhD[2,4,5,6,7,*]

[1]Cornell University, Ithaca, New York, USA. [2]Department of Brain and Cognitive Sciences, University of Rochester Medical Center, New York, USA. [3]Department of Imaging Sciences, University of Rochester Medical Center, New York, USA. [4]Elaine C. Hubbard Center for Nursing Research on Aging, University of Rochester Medical Center, New York, USA. [5]Department of Psychiatry, University of Rochester Medical Center, New York, USA. [6]Department of Neuroscience, University of Rochester Medical Center, New York, USA. [7]Department of Neurology, University of Rochester Medical Center, New York, USA.

[†]These authors contributed equally to this work.

*Address correspondence to: Feng V. Lin, PhD, CogT Lab, Center for Advanced Brain Imaging and Neurophysiology, Del Monte Institute for Neuroscience, University of Rochester Medical Center, 430 Elmwood Ave, Rochester, NY 14620, USA. E-mail: FengVankee_Lin@urmc.rochester.edu

Received: May 18, 2020; Editorial Decision Date: March 10, 2021

Decision Editor: Anne B. Newman, MD, MPH, FGSA

Abstract

Background: Perceived fatigue is among the most common complaints in older adults and is substantially influenced by diminished resources or impaired structure of widespread cortical and subcortical regions. Alzheimer's disease and its preclinical stage—mild cognitive impairment (MCI)—are considered a brain network disease. It is unknown, however, whether those with MCI will therefore perceive worse fatigue, and whether an impaired global brain network will worsen their experience of fatigue.

Methods: In this pilot case–control study of age-, sex-, and education-matched MCI and their cognitively healthy counterparts (HCs), perceived fatigue was measured using Multidimensional Fatigue Inventory, and diffusion tensor imaging tractography data were analyzed using graph theory methods to explore small-worldness properties: segregation and integration.

Results: Perceived fatigue was more severe in MCI than HCs. Despite a trend for greater network alterations in MCI, there were no significant group differences in integration or segregation. Greater perceived fatigue was related to higher segregation across groups; more perceived fatigue was related to higher segregation and lower integration in MCI but not HCs.

Conclusion: Findings of this study support the notion that altered whole-brain small-worldness properties in brain aging or neurodegeneration may underpin perceived fatigue.

Keywords: Integration, Mild cognitive impairment, Perceived fatigue, Segregation, Small worldness

Fatigue is a broad construct related to feelings of extreme tiredness and low energy, which is associated with difficulty in performing tasks (1). Increased perceived fatigue is a characteristic of aging (2) and has been linked to negative functional outcomes in older adults, suggesting it may provide a link between brain aging and daily life challenges in both healthy aging and dementia (3). Emerging notions suggest that, rather than a singular neural indicator, a distributed network of brain regions may underpin perceived fatigue (4,5). A recent expansion of computational techniques aiming to understand the organization of the whole brain as a network shows that efficient processing relies on a balance between segregation and integration at the global level (6). These graph-theoretical approaches hold promise for understanding concepts that lack clear regional bases but may represent emergent properties of disrupted whole-brain information processing, such as fatigue (7). Older adults at risk for dementia (eg, mild cognitive impairment [MCI]) show increased global segregation and reduced integration compared to their cognitively healthy counterparts (HCs), and this pattern is even more

evident in dementia (8). Additionally, this same pattern of increased segregation and decreased integration has been linked to fatigue manipulated via acute tasks in young adults (9). Together, these lines of evidence suggest that perceived fatigue may represent a behavioral outcome of whole-brain network dysfunction that occurs with brain aging and may act as a link between brain aging and functional challenges in MCI and dementia. In this study, we attempted to test this by measuring fatigue in older adults with MCI and healthy controls. We also assessed whole-brain structural network properties of segregation, integration, and small worldness by applying graph theoretical methods to diffusion tensor imaging (DTI) data to understand whether these properties relate to fatigue in healthy aging and MCI.

Method

Design

A case–control cross-sectional study was conducted.

Participants

Forty-three older HCs with typical cognition (mean age ± *SD* = 72 ± 5.36, 23.26% male, mean years of education = 17 ± 2.83), as defined by Montreal Cognitive Assessment of at least 26, were selected based on the availability of their DTI and fatigue data out of recent work from our group to examine the neural profile of fatigue in community-dwelling older adults (5,10). To match for age, 51 participants with MCI were identified from a longitudinal study from our group, with a mean age ± *SD* of 72 ± 5 years; their baseline data were used in this study (3). The diagnosis of MCI has been described previously (5); briefly, all clinics providing patients followed the National Institute on Aging and Alzheimer's Association criteria when diagnosing MCI (11). Across groups, inclusion criteria included (a) aged at least 65 years, community-dwelling, English-speaking, adequate vision and hearing for testing, and unimpaired color vision; (b) 15-item Geriatric Depression Scale (GDS) less than 6; and (c) capacity to give consent (indexed by University of California, San Diego Brief Assessment of Capacity to Consent). Exclusion criteria included (a) disease or medication that would potentially confound with fatigue; (b) neurological or vascular disorders; (c) episode of a diagnosed and active psychiatric disorder within the past 5 years; (d) change in medication or beta-blocker dosage within the past 3 months; and (e) magnetic resonance imaging (MRI) contraindications. Written informed consent was obtained before enrollment. The study was approved by the University of Research Subjects Review Board.

Perceived fatigue

The Multidimensional Fatigue Inventory (MFI) was used to assess perceived fatigue in the past month along 5 dimensions: general fatigue, physical fatigue, mental fatigue, reduced motivation, and reduced activity (12). A perceived fatigue total score was calculated as the sum of all dimensional scores. Each dimension had a possible range of 4–28 (total range of 20–140), with higher scores indicating more fatigue. Cronbach's α was 0.85 and 0.90 for HCs and MCI, respectively, for the measurement.

Imaging Data Acquisition and Preprocessing

Imaging data were collected at the University of Rochester Center for Advanced Brain Imaging and Neurophysiology using a 3T Siemens Trio TIM scanner (Erlangen, Germany) equipped with a 32-channel receive-only head coil.

Structural MRI

High-resolution T1-weighted anatomical images were collected with TR/TE = 2530/3.44 ms, TI = 1100 ms, flip angle = 7°, 256 × 256 matrix, 1 mm^3 isotropic resolution, 1 mm slice thickness, and 192 slices.

Diffusion MRI

DTI was acquired using a 2D axial single-short dual-echo SE-EPI sequence with TR/TE = 8900/86 ms, 128 × 128 matrix, 2 mm slice thickness with no gap (60 slices for whole-brain coverage), iPAT (GRAPPA) acceleration factor = 2, 60 diffusion-weighted directions, with b = 1000 s/mm^2 with 1 average and b = 0 images with 10 averages. Raw diffusion-weighted images (DWIs) were aligned to the average b0 image using the FSL eddy correct tool (www.fmrib.ox.ac.uk/fsl) to correct for head motion and eddy current distortions. FSL Brain Extraction Tool was used to remove non-brain tissue (13). DWIs were then registered with T1 images using Advanced Normalization Tools (ANTs; http://www.picsl.upenn.edu/ANTs/).

Network Construction

Structural brain connectomes were extracted using an established structural connectome processing pipeline (for details, see Ref. (14)). Briefly, this pipeline performs angular resolution diffusion tractography with anatomical priors, registers this data to parcellated T1 anatomical images for each participant, and groups each tractography data set into bundles connecting specified regions of interest. Next, cortical, subcortical, and brainstem regions were defined on T1 images for each participant using FreeSurfer v6.0.0 (http://surfer.nmr.mgh.harvard.edu/). A total of 17 subcortical regions (excluding brainstem structures) were identified. Automated cortical parcellation was performed using the Desikan-Killiany atlas (15). From the cortical and subcortical regions, we obtained a network of 85 nodes for each participant (Supplementary Table). Mean fractional anisotropy (FA), an indicator of white matter integrity, was calculated to identify connections between node pairs. We binarized the networks by applying a fixed sparsity threshold to set the strongest 20%–30% (in intervals of 1%) of connections to 1 in the adjacency matrices, and all the remaining connections to 0. This range was selected for its established index stability, which was observed in our data, and biological plausibility (16). Because graph theory indices can be affected by the size of the graphs and the number of edges used, a sparsity threshold ensures consistency of indices when comparing HCs and MCI (17). This process yielded an 85 × 85 symmetric connectivity matrix for each participant.

Graph Theory Analysis

We performed graph-theoretical analyses on clustering coefficient, characteristic path length, and small worldness using FA, as described by Watts and Strogatz (18) with GRETNA toolbox v2.0 (19) and MATLAB 2018a.

Clustering coefficient

Clustering coefficient measures the degree to which a given node in a graph clusters with its neighboring nodes. A *higher* clustering coefficient reflects *greater* segregation. At the nodal level, the clustering coefficient is computed as:

$$C_v = \frac{2e_v}{k_v(k_v - 1)}$$

where k_v is the subgraph that contains the direct neighbors connected to node v, e_v is the total number of connections in k_v,

and $k_v(k_v - 1)$ is the maximal number of possible connections in subgraph k_v.

At the global level, the average clustering coefficient describes the extent of clustering in the entire graph by averaging the clustering coefficients across all nodes. The average clustering coefficient is calculated as:

$$C_{\text{global}} = \frac{\sum_{v=1}^{N} C_v}{N}$$

where C_v is the clustering coefficient of node v, and N is the total number of nodes in the graph.

Characteristic path length

The shortest path length measures the average shortest distance between 2 nodes in a graph. A *smaller* shortest path length reflects *higher* integration. At the nodal level, the shortest path length is calculated between a node and all other nodes as:

$$L_v = \frac{\sum_{i=1,\quad v\neq i}^{N} d_{vi}}{(N-1)}$$

where d_{vi} is the minimum number of connections linking nodes v and i, and $(N-1)$ is the maximal number of possible paths in the graph.

At the global level, the characteristic path length measures the average path length between all nodes and is calculated as:

$$L_{\text{global}} = \frac{\sum_{v\neq i}^{N} L_v}{N}$$

where L_v is the average shortest path between node v and all other nodes, and N is the total number of nodes in the graph.

Integration versus segregation

The normalized metrics served as test statistics for nonrandom network properties (20). Briefly, we generated a set of random networks (N = 500) for each connectivity matrix to obtain a null distribution (6,21). Next, we summed the ratios of average clustering coefficients for a given connectivity matrix to each of its respective random networks and averaged this value over the total number of random networks. Normalized average clustering coefficient was calculated using GRETNA by the method employed in gretna_RUN_SmallWorld.m (lines 68–69):

$$\gamma_N = \frac{C_{\text{global}}}{\frac{1}{N}\sum_{x=1}^{N} C_{r,x}}$$

where N is the total number of random networks generated, C_{global} is the average clustering coefficient, and $C_{r,x}$ is the average clustering coefficient of random network x (19).

Normalized characteristic path length was obtained using the same random networks and calculated as:

$$\lambda_N = \frac{L_{\text{global}}}{\frac{1}{N}\sum_{x=1}^{N} L_{r,x}}$$

where N is the total number of random networks generated, L_{global} is the characteristic path length, and $L_{r,x}$ is the characteristic path length of random network x.

We calculated the global metrics at each sparsity threshold and summarized each metric by computing its respective area under the curve (AUC) over the range of sparsity thresholds. The integrated AUC values of γ_N (ie, γ, a measure of segregation) and λ_N (ie, λ, a measure of integration) were used in further statistical analyses.

Validation of the small-worldness properties

Small worldness measures the ratio between segregation and integration of a network. Small worldness is quantified by comparing the average clustering coefficient and characteristic path length of a given network to its respective null model (ie, an equivalent random network that shares the same number of nodes and degree distribution) (6,21). Small worldness is calculated as:

Table 1. Background Characteristics

	MCI (n = 51)	HC (n = 43)	T or χ^2 Test, df (p†)
Age, mean (*SD*)	71.27 (6.54)	71.75 (5.36)	0.38, 92 (.70)
Male, *n* (%)	16 (31.37)	10 (23.26)	0.77, 1 (.73)
Education, mean (*SD*)	16.01 (2.35)	16.95 (2.84)	1.76, 92 (.08)
Use of beta-blockers, *n* (%)	8 (15.69)	8 (18.60)	0.14, 1 (.71)
Chronic condition index, mean (*SD*)	4.47 (2.09)	4.53 (2.13)	0.14, 92 (.88)
GDS, mean (*SD*)*	2.16 (2.32)	0.67 (1.41)	**–3.66, 92 (<.001)**
MoCA, mean (*SD*)	24.12 (2.39)	27.67 (1.69)	**8.19, 92 (<.001)**
MFI, mean (*SD*)			
Total score	58.65 (22.03)	46.74 (14.68)	**–3.02, 92 (.002)**
General fatigue	13.75 (6.22)	11.07 (3.91)	**–2.44, 92 (.016)**
Physical fatigue	11.64 (6.09)	8.72 (3.70)	**–2.75, 92 (.007)**
Reduced activity	10.94 (5.12)	8.34 (4.43)	**–2.29, 92 (.024)**
Reduced motivation	9.88 (5.12)	7.16 (3.58)	**–2.93, 92 (.004)**
Mental fatigue	12.43 (5.70)	11.44 (5.33)	–0.86, 92 (.39)
Small-worldness measures, mean (*SD*)			
Segregation (γ)		0.1657 (9.60e-3)	1.46, 92 (.15)
Integration (λ)	0.1036 (6.70e-4)	0.1034 (5.90es-4)	1.50, 92 (.14)

Note: MCI = mild cognitive impairment; HCs = healthy controls; GDS = Geriatric Depression Scale; MoCA = Montreal Cognitive Assessment; MFI = Multidimensional Fatigue Inventory. Bold values indicate statistical significance at $p < 0.05$.

*Item "Do you feel full of energy?" was removed from GDS.

†p values across MFI subdomains were FDR-corrected.

$$\sigma = \frac{\gamma_N}{\lambda_N}$$

where γ_N is the normalized average clustering coefficient and λ_N is the normalized characteristic path length of random network x. A network is considered to have small-worldness properties if σ greater than 1. We calculated γ_N, λ_N, and σ at each sparsity threshold (ie, 20%–30% in an interval of 1%). All participants possessed small-worldness properties (σ > 1) across all sparsity thresholds, suggesting the validity of applying integration and segregation indices. Although Telesford et al. (22) have described a newer measure of small worldness that is more stable across different graph sizes, we chose this methodology because σ greater than 1 is an established characteristic of small-world brain networks, and increased stability across graph sizes was not necessary because the same 85 nodes were used for each participant (20).

Other Measures

Depressive symptoms were measured using the 15-item GDS. One question (ie, "Do you feel full of energy?") was removed due to its similarity in assessing fatigue (23). All positive items were summed. We also collected data on beta-blocker use and the presence of chronic health conditions (24). All main variables of the study are presented in Table 1.

Statistical Analyses

Group comparisons of background characteristics were performed using two-sample *t*-tests for continuous measures and chi-square tests for categorical measures. Associations between continuous variables were quantified using Spearman's rank correlation. Statistical significance was evaluated at α = 0.05. Analyses were primarily focused on whole-brain graph measures of small worldness and total MFI score and secondarily on regional small-worldness measures and MFI domain subscores with false discovery rate (FDR) correction. All statistical analyses were performed using MATLAB 2018a.

Results

Group Comparisons for Graph Characteristics, Small-Worldness Measures, and Perceived Fatigue

Average mean FA across the entire brain was not found significantly different between HCs and MCI. These nonsignificant results indicate that the sparsity threshold did not influence group difference in the graph measures. There was no group difference in segregation (γ) or integration (λ) although we did observe a trend for both higher γ (p = .14) and λ (p = .15) in MCI compared to HCs. Perceived fatigue was higher in MCI compared to HCs for total MFI score, as well as the subdomains, excluding mental fatigue (Table 1).

Relationship Between Small-Worldness Measures and Perceived Fatigue

Higher perceived fatigue was related to higher segregation (ie, higher γ) for the entire sample. When conducting within-group analysis, higher perceived fatigue was related to higher segregation and lower integration (ie, higher λ) in MCI but not HC (Figure 1). No nodal level graph metrics in relation to fatigue survived FDR correction in the entire sample or within the group. When controlling for confounders (ie, GDS, AD signature cortical thickness, use of beta-blockers, and chronic condition index), the findings for the MCI group remained significant.

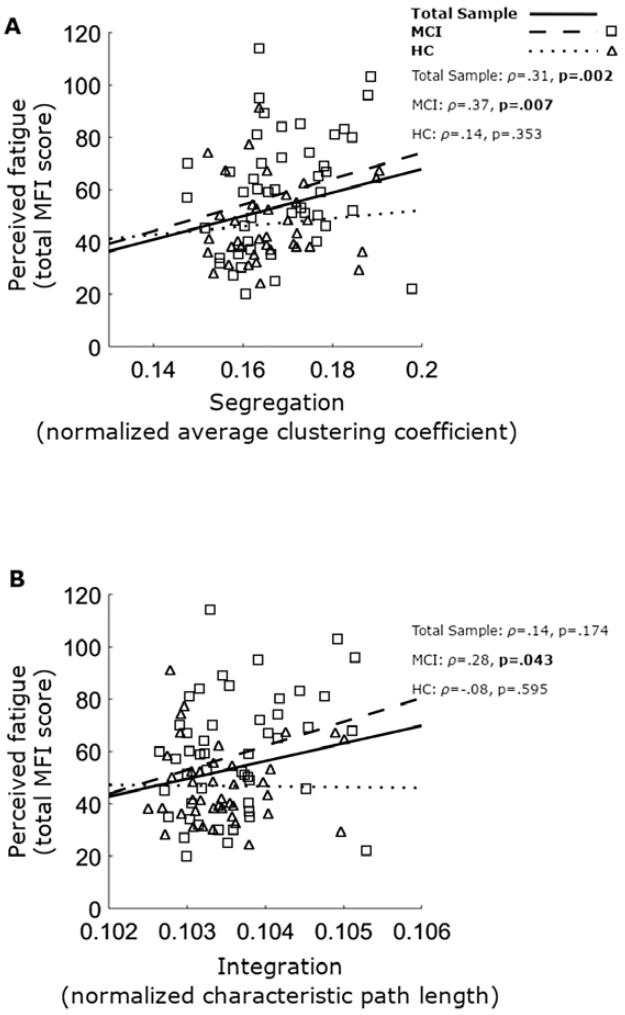

Figure 1. Scatterplots of perceived fatigue versus global small-worldness properties. (**A**) Correlation between perceived fatigue and segregation for the total sample (solid line), MCI (dashed line, squares), and HCs (dotted line, triangles). Perceived fatigue (y-axis) was measured as the sum of the MFI dimensional scores. Higher scores indicate greater perceived fatigue. Segregation (x-axis) was indexed as normalized average clustering coefficient (γ). Higher values of γ indicate greater segregation. (**B**) Correlation between perceived fatigue and integration. Integration (x-axis) was indexed as normalized characteristic path length (λ). Lower values of λ indicate greater integration. MFI = Multidimensional Fatigue Inventory; MCI = mild cognitive impairment; HCs = healthy controls.

Because the MFI fatigue score was derived from 5 subdomain scores, we also examined the relationships between small-worldness measures and individual fatigue domains (Table 2). With FDR correction, higher fatigue scores in all subdomains, except mental fatigue, were significantly correlated with higher segregation in the entire sample.

Discussion

The main findings of this study were that (a) perceived fatigue, both total and subdomain scores, except mental fatigue, was more severe in MCI compared to HCs; (b) both MCI and HC groups possessed small-worldness properties, but despite a trend for greater network alterations in MCI, there were no significant group differences in

Table 2. Correlations Between Fatigue Domains and Global Small-Worldness Properties

	MFI Domain	γ	λ
		Spearman's ρ, R^2, *df* (*p**)	
MCI (*n* = 51)	**Total score**	**0.37, 0.137, 49 (.007)**	**0.28, 0.078, 49 (.043)**
	General fatigue	0.27, 0.073, 49 (.05)	0.23, 0.053, 49 (.10)
	Physical fatigue	**0.35, 0.123, 49 (.009)**	0.23, 0.053, 49 (.09)
	Reduced activity	0.27, 0.073, 49 (.05)	0.16, 0.026, 49 (.24)
	Reduced motivation	0.26, 0.068, 49 (.06)	**0.29, 0.084, 49 (.041)**
	Mental fatigue	0.18, 0.032, 49 (.20)	0.08, 0.006, 49 (.53)
HC (*n* = 43)	**Total score**	0.14, 0.023, 41 (.35)	−0.08, 0.006, 41 (.59)
	General fatigue	0.04, 0.001, 41 (.76)	−0.12, 0.014, 41 (.41)
	Physical fatigue	0.01, 1e-4, 41 (.90)	0.04, 0.002, 41 (.75)
	Reduced activity	0.14, 0.020, 41 (.34)	0.07, 0.005, 41 (.62)
	Reduced motivation	0.20, 0.040, 41 (.18)	−0.04, 0.002, 41 (.76)
	Mental fatigue	−0.04, 0.002, 41 (.80)	−0.02, 4e-4, 41 (.15)
Combined sample (*n* = 94)	**Total score**	**0.31, 0.096, 92 (.002)**	0.14, 0.020, 92 (.17)
	General fatigue	**0.21, 0.044, 92 (.044)**	0.08, 0.006, 92 (.40)
	Physical fatigue	**0.25, 0.063, 92 (.016)**	0.17, 0.029, 92 (.09)
	Reduced activity	**0.25, 0.063, 92 (.016)**	0.15, 0.023, 92 (.15)
	Reduced motivation	**0.27, 0.073, 92 (.009)**	0.16, 0.026, 92 (.12)
	Mental fatigue	0.09, 0.008, 92 (.36)	−0.03, 9e-4, 92 (.75)

Note: γ = segregation (normalized average clustering coefficient); λ = integration (normalized characteristic path length); MCI = mild cognitive impairment; HC = healthy controls; MFI = Multidimensional Fatigue Inventory. Bold values indicate statistical significance at $p < 0.05$.

**p* values across MFI subdomains were FDR-corrected.

integration or segregation; (c) greater perceived fatigue was related to higher segregation across groups; and (d) greater perceived fatigue was related to higher segregation and lower integration in MCI but not HCs.

Findings of the present study support the notion that altered whole-brain small-worldness properties in brain aging or neurodegeneration may underpin perceived fatigue. A loss of connections driven by advancing age or pathology alters network topology and the dynamics between different networks. These changes elicit progressively disruptive changes in information transfer critical for distributed processes, such as perceived fatigue. Because MCI is a condition driven by exaggerated brain aging or pathology (11), the findings of worse fatigue, as well as a more evident relationship between perceived fatigue and altered small-worldness properties in MCI, further support this notion. Findings from Lin et al. (25) suggest that global graph theory measures are more sensitive to changes in structural network topology in MCI than in HCs. Additionally, He et al. (17) have described how small-worldness measures are vulnerable to attacks on localized subsets of regions, which are known to occur during the progression of Alzheimer's disease (AD). Our findings align with this literature and suggest that graph measures in MCI are more vulnerable to fatigue-related alterations in network topology than in HCs. We suggest that heightened vulnerability of graph measures may explain the correlations we observed between small worldness and perceived fatigue measures for MCI but not HC. Also of note, He et al. (17) reported significantly higher segregation and lower integration in AD compared to HCs. The insignificant but trending group difference in small-worldness properties of this study may be explained by less severe brain pathology in MCI compared to AD. However, the causality between fatigue and small worldness needs to be further corroborated in future studies. It is unclear whether there is a shared etiology explaining both aspects, such as the possibility that hypermetabolism relates to both fatigue and brain network dysfunction, or whether complaints of fatigue are a byproduct of a global network deficiency.

Limitations need to be acknowledged. First, this study was based on data drawn from another clinical investigation. As a result, this study had a relatively low sample size and did not include exhaustive measures of fatigue. These results should therefore be treated as preliminary findings to guide future work. Second, we used the MFI, a measure of trait fatigue in the past month. Differentiating the 5 dimensions of trait fatigue may be of restricted use, given the relatively underdeveloped validity of the dimensional scores in the measure. However, our recent work does provide evidence of a shared white matter mechanism underlying physical and cognitive fatigue (5). Third, it is unclear whether the current relationship would remain when examining fatigability (ie, acute fatigue response to fatigue manipulation tasks), which is another critical aspect of fatigue. Finally, we did not examine any AD pathologies (eg, amyloid, p-tau) in the context of MCI. Examining these aspects may provide additional insight in determining whether the etiology of fatigue complaints is unique to AD pathology or general age-related neurodegeneration.

Supplementary Material

Supplementary data are available at *The Journals of Gerontology, Series A: Biological Sciences and Medical Sciences* online.

Funding

The study was supported by the National Institutes of Health (R01NR015452 and R21AG053193 to F.V.L.).

Conflict of Interest

None declared.

References

1. Kluger BM, Krupp LB, Enoka RM. Fatigue and fatigability in neurologic illnesses: proposal for a unified taxonomy. *Neurology*. 2013;80:409–416. doi:10.1212/WNL.0b013e31827f07be
2. Eldadah BA. Fatigue and fatigability in older adults. *PM R*. 2010;2:406–413. doi:10.1016/j.pmrj.2010.03.022
3. Lin F, Chen DG, Vance DE, Ball KK, Mapstone M. Longitudinal relationships between subjective fatigue, cognitive function, and everyday functioning in old age. *Int Psychogeriatr*. 2013;25:275–285. doi:10.1017/S1041610212001718
4. Goñi M, Basu N, Murray AD, Waiter GD. Neural indicators of fatigue in chronic diseases: a systematic review of MRI studies. *Diagnostics*. 2018;8:42. doi:10.3390/diagnostics8030042
5. Baran TM, Zhang Z, Anderson AJ, McDermott K, Lin F. Brain structural connectomes indicate shared neural circuitry involved in subjective experience of cognitive and physical fatigue in older adults. *Brain Imaging Behav*. 2019;14:2488–2499. doi:10.1007/s11682-019-00201-9
6. Sporns O, Zwi JD. The small world of the cerebral cortex. *Neuroinformatics*. 2004;2:145–162. doi:10.1385/NI:2:2:145
7. DeLuca J, Johnson SK, Natelson BH. Information processing efficiency in chronic fatigue syndrome and multiple sclerosis. *Arch Neurol*. 1993;50:301–304. doi:10.1001/archneur.1993.00540030065016
8. Dai Z, He Y. Disrupted structural and functional brain connectomes in mild cognitive impairment and Alzheimer's disease. *Neurosci Bull*. 2014;30:217–232. doi:10.1007/s12264-013-1421-0
9. Li J, Lim J, Chen Y, et al. Mid-Task break improves global integration of functional connectivity in lower alpha band. *Front Hum Neurosci*. 2016;10:304. doi:10.3389/fnhum.2016.00304
10. Rossetti HC, Lacritz LH, Cullum CM, Weiner MF. Normative data for the Montreal cognitive assessment (MoCA) in a population-based sample. *Neurology*. 2011;77:1272–1275. doi:10.1212/WNL.0b013e318230208a
11. Albert MS, DeKosky ST, Dickson D, et al. The diagnosis of mild cognitive impairment due to Alzheimer's disease: recommendations from the National Institute on Aging-Alzheimer's Association workgroups on diagnostic guidelines for Alzheimer's disease. *Alzheimers Dement*. 2011;7:270–279. doi:10.1016/j.jalz.2011.03.008
12. Smets EM, Garssen B, Bonke B, De Haes JC. The Multidimensional Fatigue Inventory (MFI) psychometric qualities of an instrument to assess fatigue. *J Psychosom Res*. 1995;39:315–325. doi:10.1016/0022-3999(94)00125-o
13. Smith SM. Fast robust automated brain extraction. *Hum Brain Mapp*. 2002;17:143–155. doi:10.1002/hbm.10062
14. Zhang Z, Descoteaux M, Zhang J, et al. Mapping population-based structural connectomes. *Neuroimage*. 2018;172:130–145. doi:10.1016/j.neuroimage.2017.12.064
15. Desikan RS, Ségonne F, Fischl B, et al. An automated labeling system for subdividing the human cerebral cortex on MRI scans into gyral based regions of interest. *Neuroimage*. 2006;31:968–980. doi:10.1016/j.neuroimage.2006.01.021
16. Dennis EL, Jahanshad N, Rudie JD, et al. Altered structural brain connectivity in healthy carriers of the autism risk gene, CNTNAP2. *Brain Connect*. 2011;1:447–459. doi:10.1089/brain.2011.0064
17. He Y, Chen Z, Evans A. Structural insights into aberrant topological patterns of large-scale cortical networks in Alzheimer's disease. *J Neurosci*. 2008;28:4756–4766. doi:10.1523/JNEUROSCI.0141-08.2008
18. Watts DJ, Strogatz SH. Collective dynamics of 'small-world' networks. *Nature*. 1998;393:440–442. doi:10.1038/30918
19. Wang J, Wang X, Xia M, Liao X, Evans A, He Y. GRETNA: a graph theoretical network analysis toolbox for imaging connectomics. *Front Hum Neurosci*. 2015;9:386. doi:10.3389/fnhum.2015.00386
20. Bassett DS, Bullmore ET. Small-world brain networks revisited. *Neuroscientist*. 2017;23:499–516. doi:10.1177/1073858416667720
21. Haneef Z, Levin HS, Chiang S. Brain graph topology changes associated with anti-epileptic drug use. *Brain Connect*. 2015;5:284–291. doi:10.1089/brain.2014.0304
22. Telesford QK, Joyce KE, Hayasaka S, Burdette JH, Laurienti PJ. The ubiquity of small-world networks. *Brain Connect*. 2011;1:367–375. doi:10.1089/brain.2011.0038
23. Marc LG, Raue PJ, Bruce ML. Screening performance of the 15-item geriatric depression scale in a diverse elderly home care population. *Am J Geriatr Psychiatry*. 2008;16:914–921. doi:10.1097/JGP.0b013e318186bd67
24. Swain MG. Fatigue in chronic disease. *Clin Sci (Lond)*. 2000;99:1–8. doi:10.1042/cs0990001
25. Lin SY, Lin CP, Hsieh TJ, et al. Multiparametric graph theoretical analysis reveals altered structural and functional network topology in Alzheimer's disease. *Neuroimage Clin*. 2019;22:101680. doi:10.1016/j.nicl.2019.101680